An Evaluation of a High-Resolution Hydrometeorological Modeling System for Prediction of a Cool-Season Flood Event in a Coastal Mountainous Watershed

KENNETH J. WESTRICK AND CLIFFORD F. MASS

Department of Atmospheric Sciences, University of Washington, Seattle, Washington

(Manuscript received 11 August 1999, in final form 9 August 2000)

ABSTRACT

This study used the atmospheric Fifth-Generation Pennsylvania State University–National Center for Atmospheric Research Mesoscale Model (MM5) and the University of Washington Distributed Hydrology–Soil–Vegetation Model (DHSVM) for the simulation of a complex rain-on-snow flood event that occurred from 28 December 1996 to 3 January 1997 on the 1560-km^2 Snoqualmie River watershed in western Washington. Three control simulations were created with MM5 applied at 36-, 12-, and 4-km horizontal spacing and DHSVM at a horizontal spacing of 100 m. Results showed that the accuracy of the atmospheric fields increased with higher horizontal resolution, although underforecasting of precipitation was evident for all three resolutions. Simulated river flows captured 67% (36 km), 75% (12 km), and 72% (4 km) of the total flow and 52% (36 km), 58% (12 km), and 62% (4 km) of the event peak flow.

Several sensitivity simulations of the modeling system (4-km spacing only) were conducted to improve on the control simulations. Adjusting the MM5 precipitation using observations led to a streamflow forecast that captured 90% of the total flow. Reduction of the model high–wind speed bias improved the simulated snowmelt, although the resulting effects on streamflow were relatively small. A sensitivity experiment that included the precipitation from an intense rainband that was not captured by MM5 revealed the importance of this high-intensity, short-lived feature; simulated streamflow from this experiment captured 93% of the total flow and over 82% of the peak flow, with a 4-h timing error.

A final set of sensitivity simulations, using both a higher- and lower-elevation observation as the sole forcing of DHSVM (no MM5), revealed strong sensitivity to the observation location; using a slightly displaced (~8 km) lower-elevation observation produced river flows that differed by over 18%. Both of the resulting simulated river flows forced by the two-station method were significantly lower than both the observed flows (35% and 53% of total observed flow) and the flows simulated with the MM5 input fields. A major cause of this low flow was that the temperatures at the observation locations were located in gap regions of the Cascade Mountains, were not representative of the basin-average temperature, and therefore caused too much precipitation to fall as snow.

1. Introduction

Between 1990 and 1996, 12 major wintertime flooding events on the west coast of the United States have resulted in more than $2.4 billion in damage and the loss of at least 55 lives, as variously reported in *Storm Data*. Much of the increase in damage and death can be attributed to growth in population and the resulting flood plain development. Urbanization has changed the timing, magnitude, volume, and duration of flood events, resulting in larger volumes of runoff and a decrease in the time to peak (Urbonas and Roesner 1993). Extensive road networks in mountainous areas, combined with the effect of tree harvesting, have increased storm flow volume, peak flow, and storm flow duration (Calder 1993). As populations continue to grow in the western United States, and the land cover is increasingly altered, the need for accurate forecasting of flood events becomes increasingly important.

Physically based, distributed hydrological models are suitable for flood forecasting in the Pacific Northwest because they can represent the spatial heterogeneity in basin characteristics and input, such as precipitation. A number of research studies using distributed hydrological models in the Pacific Northwest of the United States have highlighted the importance of accurate meteorological fields for achieving physically reasonable hydrological solutions (Bowling et al. 2000; Storck et al. 1998). Atmospheric mesoscale models, which have progressed rapidly in the past 10 years, have been shown to produce accurate regional forecasts of precipitation and other meteorological fields when forced with realistic large-scale conditions. This study focuses on the direct use of high-resolution mesoscale atmospheric model data to force a distributed hydrological model for

Corresponding author address: K. J. Westrick, Atmospheric Sciences, Box 351640, University of Washington, Seattle, WA 98195.
E-mail: westrick@atmos.washington.edu

the forecasting of a complex rain-on-snow (ROS) flood event, with an emphasis on the evaluation and sensitivities of the meteorological components of the system.

2. Background

Precipitation is arguably the most important meteorological component for forcing a hydrologic model for flood forecasting. Unfortunately, determining accurate precipitation distributions in mountainous regions is difficult because of the spatial nonuniformity of the precipitation, which is heavily influenced by the orography. The regional coverage of rain gauges is relatively coarse, and much of the data is not available in real time. The network of Weather Surveillance Radars-1988 Doppler (WSR-88D) is also of limited use because of complications ranging from uncertainties in the radar reflectivity–rainfall rate (Z–R) relationship to brightband contamination. Even when many of the radar's problems are mitigated, the effective coverage of the radar for quantitative precipitation measurement during the cool season is limited to only one-third of the land surface in the coastal western United States (Westrick et al. 1999). Mesoscale atmospheric models are a possible method for providing high-resolution meteorological forecast fields to a hydrological model. These model fields could be augmented with available real-time observational data to create improved spatially continuous precipitation fields. Mesoscale atmospheric models can be used for forecasting future conditions, thus providing longer lead times to prepare for potentially damaging floods. Of course, mesoscale models have potential problems too, such as poor initialization, inadequate resolution, and deficiencies in model physics.

Atmospheric models have been used previously to force hydrological models for short-term river flow prediction. For example, the Pennsylvania State University–National Center for Atmospheric Research (PSU–NCAR) Mesoscale Model, version 4 (MM4), was used to force the U.S. Army Corps of Engineers Hydrologic Engineering Center (HEC-1) hydrological model (Warner et al. 1991). Ten precipitation events, mainly winter and spring season, were simulated for the flood-prone Susquehanna River basin in New York and Pennsylvania. In general, this system overpredicted basin precipitation and river flow, although the authors suggested that the overprediction was at least partially attributable to relatively coarse MM4 horizontal resolution (60 km spacing) and deficiencies in the convective parameterization scheme.

Miller and Kim (1996) coupled the Mesoscale Atmospheric Simulation model to the distributed hydrological model ''TOPMODEL'' to simulate a 1995 flooding event on the flood-prone Russian River of northern California. This case was typical of most major West Coast cool-season flooding events, with several separate storms striking in quick succession. Results from the study indicated that soil texture, topography, and initial soil water saturation deficit were the most important *surface* properties for computing river flow. However, the simulated total discharge over the 12-day event was approximately 50% greater than observed [Fig. 6 of Miller and Kim (1996)], suggesting a significant overprediction of precipitation.

Several studies have shown that decreasing the horizontal grid spacing of the atmospheric model enhances accuracy in simulating precipitation, especially in mountainous regions. Colle and Mass (1996) showed improvements in the Fifth-Generation PSU–NCAR Mesoscale Model (MM5) precipitation fields over the Olympic Mountains of Washington when model horizontal spacing was decreased from 27 to 3 km. Katzfey (1995) noted improvements in the simulated precipitation produced by the Division of Atmospheric Research limited-area model when horizontal spacing was decreased from 30 to 15 km. Martin (1996) showed that the National Centers for Environmental Prediction (NCEP) Meso Eta Model (29 km) provided superior quantitative precipitation forecasts when compared with the lower-resolution NCEP Nested Grid Model for a 1995 winter flooding event in California and attributed this result mainly to the more realistic representation of terrain in the Meso Eta Model.

Another factor complicating ROS floods is that a significant amount of the runoff is from snowmelt. For example, during the Oregon flood of February 1996, Taylor (1997) found that over one-third of the total water input to the river network was from snowmelt. Van Heeswijk et al. (1996) examined the relative importance of energy fluxes involved in snowmelt and found that, during an ROS flooding event in the Washington Cascade Range over half the energy input to the snowpack was from sensible and latent heat fluxes. Because both of these depend strongly on temperature and wind speed, this result underscores the importance of accurately forecasting these fields. Several studies have shown that accurate wind and temperature fields can be simulated in complex terrain if the horizontal resolution captures the principle orography (Steenburgh et al. 1997; McQueen et al. 1995).

This paper assesses the performance of a streamflow forecast system that uses output from MM5 to drive a distributed hydrology model (Wigmosta et al. 1994) for the prediction of a Pacific Northwest cool-season flood event. The specific objectives of this study are

1) to determine the ability of the system to predict river flow on a coastal mountainous watershed during a single cool-season flood event,
2) to assess the importance of atmospheric model horizontal grid spacing on the accuracy of the various meteorological fields and the subsequent effect on simulated river flows, and
3) to identify weaknesses in the simulation and to conduct sensitivity studies on meteorological compo-

nents that were suspected to cause the greatest degradation of the simulation.

This paper is organized as follows: A brief description of the local geography is covered in section 2, followed in section 3 by a description of the atmospheric and hydrological models and the hydrological model initialization. A case overview is presented in section 4, with model results covered in section 5. Section 6 reviews the results of various sensitivity experiments, with a summary and recommendations in section 7.

3. Geographical and model description

The area chosen for this study is the Snoqualmie River watershed, located on the western flanks of the Cascade Range of mountains just east of Seattle, Washington (Fig. 1a). The western third of the 1560-km^2 basin is relatively flat, at low elevation, and primarily nonforested; the eastern two-thirds are characterized by steep orography with thick conifer forests interspersed with clear cuts (Fig. 1b). In addition to several in situ observation sites, a WSR-88D is located approximately 80 km to the northwest, at Camano Island, and a wind profiler is positioned 25 km west of Carnation in northeast Seattle (Fig. 1a). The Carnation river flow gauge is used for flow verification in the study. In the 69-yr flow record for this gauge, the extreme maximum discharge was 1850 m^3 s^{-1} (65 200 ft^3 s^{-1}), and the average annual streamflow was 2139 mm yr^{-1} (84.22 in. yr^{-1}). This basin is flood prone, with a vast majority of the floods occurring between late October and early March. Most of the flood events are due to prolonged, moderate rainfall, often combined with significant low to midelevation snowmelt.

a. Atmospheric model: MM5

MM5 is a sigma-coordinate mesoscale atmospheric model (Grell et al. 1995) that has been used extensively for both research and forecasting throughout the world. For this study, the model was run nonhydrostatically over an outer grid and two nested grids with horizontal spacing of 36, 12, and 4 km, respectively (Fig. 2). Thirty-two vertical layers were used, with increased resolution in the planetary boundary layer (PBL). Initial and boundary conditions, available at 6-h intervals, were interpolated from the NCEP Eta Model ''104'' grids (80-km horizontal/25-hPa vertical spacing) to the MM5 grid. Some MM5 physics options used were

- the simple-ice, explicit-microphysics scheme (Dudhia 1989),
- the Blackadar high-resolution PBL scheme (Zhang and Anthes 1982),
- the Kain–Fritsch cumulus parameterization applied only on the 36- and 12-km domains (Kain and Fritsch 1990), thus assuming that convection will be resolved explicitly with the 4-km-spacing nest, and
- longwave and shortwave radiation schemes that account for interactions among the atmosphere, clouds, precipitation fields, and the surface (Dudhia 1989).

The differences in MM5 model terrain over the Snoqualmie watershed at the various atmospheric model resolutions are shown in Figs. 1c,d,e. The major Cascade gaps and the main tributaries of the river network are at least partially resolved at a model horizontal spacing of 4 km (Fig. 1e). The effect of model horizontal spacing on the average terrain cross section is shown in Fig 1f. At 36-km horizontal spacing, the effective height of the barrier near crest level is only 81% of the actual average height of the barrier. Better representation is noted when spacing is decreased to 12 km (98% of actual average barrier height), and at 4 km the average crest-level height is 99% of actual with an improved representation of the terrain slope.

A total of 10 simulations, initialized every 12 h between 1200 UTC 28 December 1996 and 0000 UTC 2 January 1997, were completed (Fig. 3). This approach was used for two reasons: First, the forecasts essentially mirror those that would have been available in real time to forecasters (if this system were used operationally). Second, reinitializing the atmospheric model with more accurate initial states reduces the total error that would have accumulated over the relatively long 132-h forecast period. In all of the atmospheric simulations, the 13–24-h atmospheric forecast, which has been shown to be the most accurate with regard to precipitation (Colle et al. 1999), was used to force the hydrological model. To maintain the focus on the potential use of this kind of system for operational forecasting, four-dimensional data assimilation and observational nudging were not used.

b. Hydrological model: DHSVM

The Distributed Hydrology–Soil–Vegetation Model (DHSVM) is a physically based, distributed hydrological model developed for use in complex terrain (Wigmosta et al. 1994). The model accounts explicitly for the spatial distribution of land surface processes at high resolution. Downslope moisture redistribution in the saturated zone is based on the local topographic slope. Return and saturation overland flow are generated in locations where the gridcell water tables intersect the ground surface. The model includes the effects of both a vegetative understory and an overstory. Evapotranspiration from vegetation is modeled using a Penman–Monteith approach. Solar radiation and wind speed are attenuated through the two canopies based on vegetation cover density and leaf area index.

For establishing the snow distribution, a linear transition between a lower-threshold temperature (-0.5°C), below which all precipitation is snow, and an upper-threshold temperature (1.0°C), above which all precipitation is rain, is used. For this study, DHSVM was run

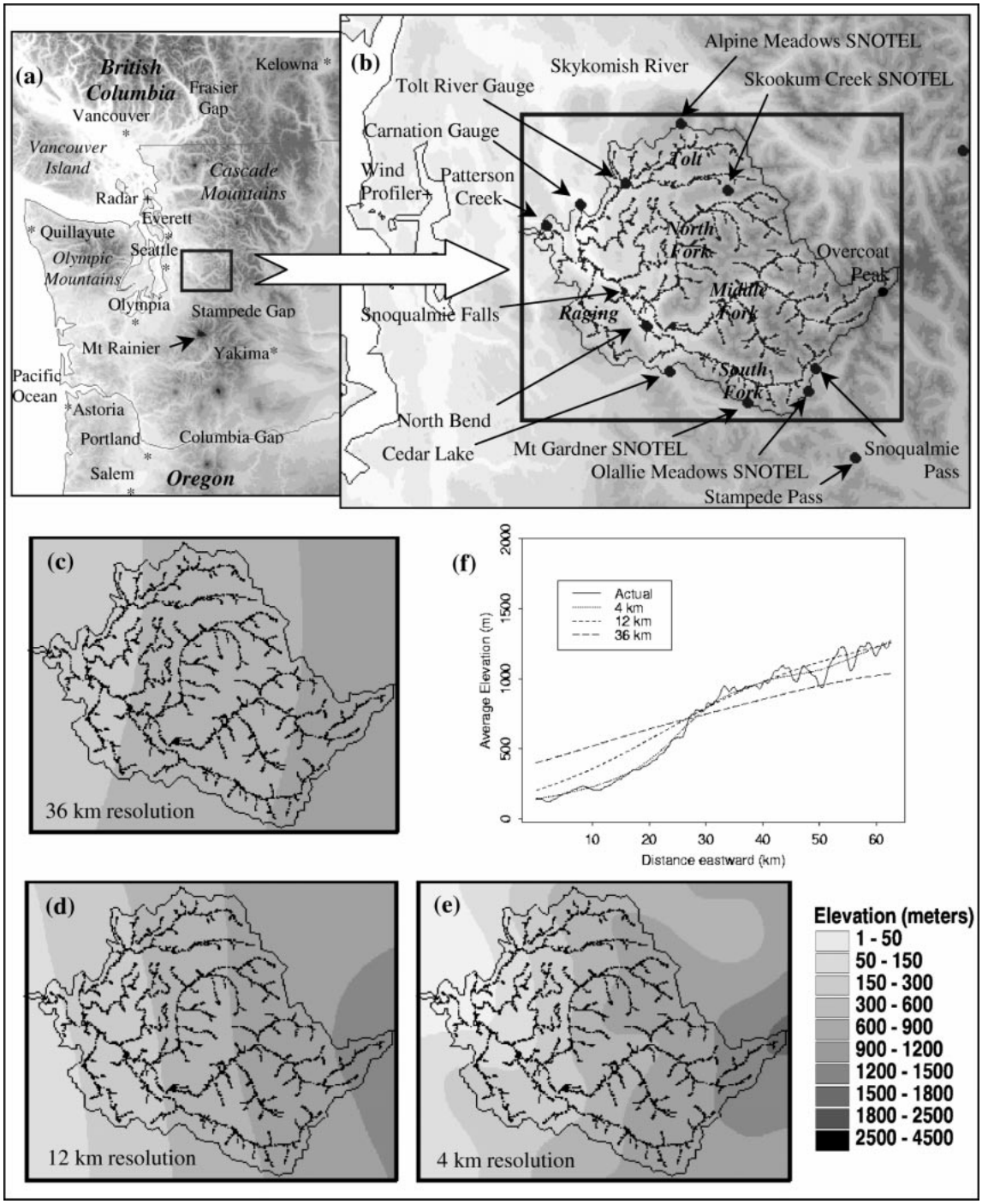

FIG. 1. Relief map of (a) the Pacific Northwest, (b) the Snoqualmie River basin, the atmospheric model terrain over the Snoqualmie basin at (c) 36-, (d) 12-, and (e) 4-km spacing, and (f) a west–east cross section showing the average terrain profile for the various MM5 model resolutions and the actual terrain, taken from a 100-m horizontal-spacing digital elevation map.

at 100-m horizontal spacing and included 9 soil and 19 land use types. A distributed-velocity routing model (Maidment et al. 1996) was used to determine the travel time of the return and overland flow from the originating pixel to the basin outlet. The effect of canopy snow interception on ground snowpack accumulation is explicitly represented. The hydrological model had been previously applied to this watershed to study the effects of land use changes (Storck et. al. 1995), and the reader is referred to this work for details on the calibration.

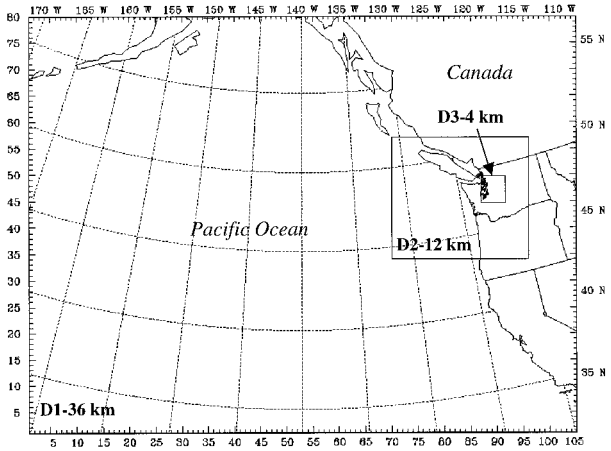

FIG. 2. Location and horizontal spacing of the three domains used for the MM5 atmospheric simulations.

c. Model interface

A total of eight separate meteorological fields are required by DHSVM. Temperature, humidity, wind speed, incident shortwave and longwave radiation, and surface pressure are interpolated from the MM5 grid points to the 100-m spacing of the DHSVM grid using biparabolic interpolation. The MM5 precipitation field is interpolated to the DHSVM grid using the method of Cressman (1959). To account for the temperature difference between the model and actual surface elevation, the MM5 mean lapse rate in the 150-hPa-thick layer above the model-predicted PBL is determined and applied to the difference between the actual and model terrain height. Because of the relatively small size of the basin (with respect to the atmospheric model domain) and the strong meteorological forcing, feedback from the hydrological model back to the atmospheric model was considered to be negligible and, therefore, was neglected.

d. Hydrological model initialization

Based on findings from previous research that revealed the importance of antecedent conditions (Miller and Kim 1996), a multiyear initialization of DHSVM was performed. Two years of meteorological observations from Stampede Pass, taken from the statistically average water year 1989/90, were used to initialize the hydrological model to the conditions assumed to be rep-

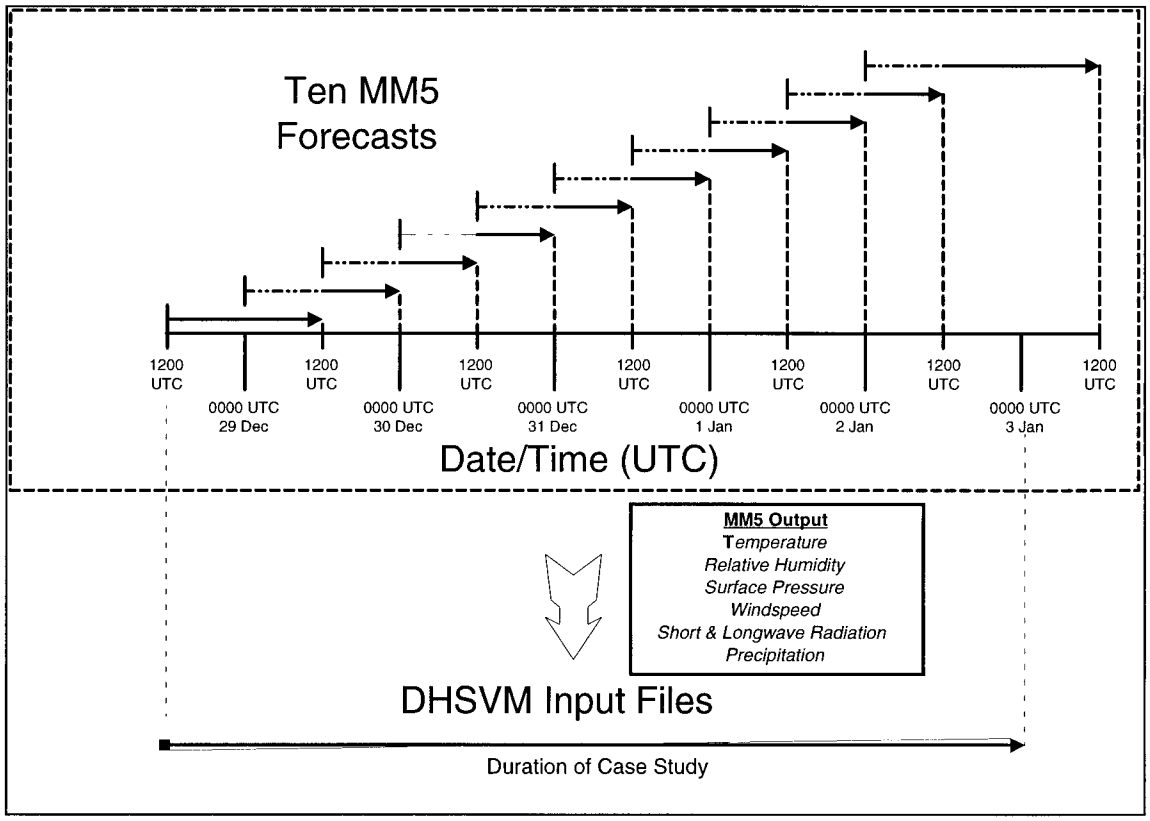

FIG. 3. Schematic describing how the MM5 simulations were used to create input fields for DHSVM. Ten MM5 simulations initialized every 12 h between 1200 UTC 28 Dec 1996 and 0000 UTC 2 Jan 1997 were used to create the DHSVM input data. To allow for the ''spinup'' of the MM5 precipitation fields, the 13–24-h forecasts were used (solid portion of arrows at top of schematic).

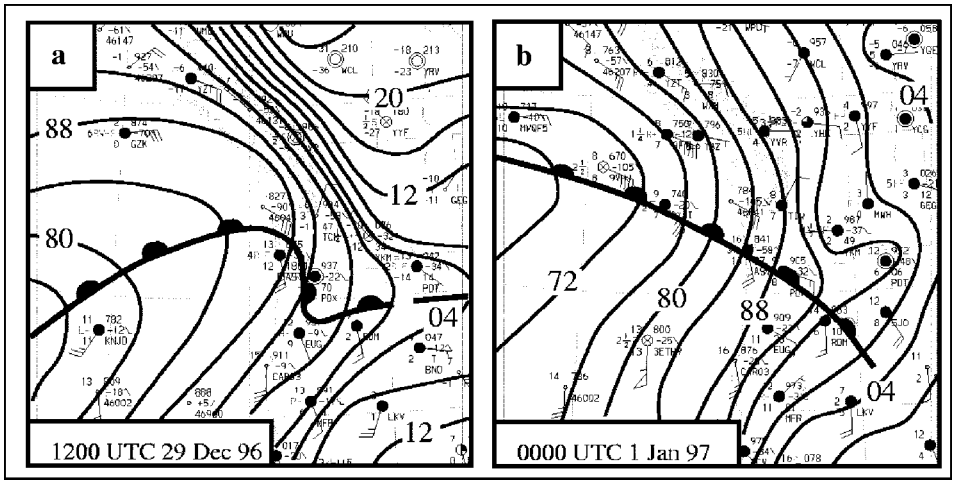

FIG. 4. Surface analysis for (a) 1200 UTC 29 Dec 1996 and (b) 0000 UTC 1 Jan 1997.

resentative of 1 July 1996. From 1 July through 28 December 1996, actual meteorological observations from the Stampede Pass automated surface observation system and an observation site in North Bend (Fig. 1b) were used as forcing.

Using these two stations, the predicted total discharge between 1 October and 28 December 1996 was approximately 77% of observed at the Carnation river gauge site. Because snow water equivalent (SWE) values over the basin were also low, it was concluded that there was insufficient model precipitation during the spinup period. This is most likely due to the two observations not being representative of the mean areal precipitation. Therefore, to improve the initial fields and insure a water mass balance, precipitation values for the period 1 October through 28 December were multiplied by the factor 1.3 (1.0/0.77), which effectively eliminated the average-flow bias and brought the initial model snow fields to within 15% of observed. To further improve the initial SWE field, a correction toward observations was performed. Using snowpack telemetry (SNOTEL) and other observations, an enhancement ratio, defined as the ratio of observed to model-predicted SWE, was determined and was used to modify the SWE at each grid point. The correction was applied spatially to the SWE field using a method similar to that of Stauffer and Seaman (1994), which reduces the weighting of the observation as a function of both vertical and horizontal distance.

4. Case overview

The time period for the case study is from 1200 UTC 28 December 1996 through 0000 UTC 3 January 1997. At the beginning of this event, a snowpack existed over the entire Snoqualmie watershed, with 25–50 cm (10–20 in.) of snow over the lower elevations ($<$200 m) and significantly greater amounts ($>$3 m) reported at many higher-elevation locations ($>\sim$500 m). A snowpack is common at the higher elevations at this time of year, but a significant snowpack at lower elevations is unusual.

The first weather system passed through the region on 29–30 December 1996. The surface analysis for 1200 UTC 29 December (Fig. 4a) shows a warm front extending to the coast in the vicinity of the Washington–Oregon border. Extremely cold air east of the Cascades retarded the progression of the surface front, and the Camano Island WSR-88D detected strong easterly flow through the major gaps in the Cascade Range (Fig. 5a). At the Sand Point (Seattle) wind profiler a wind shift marked the passage of the warm front at the 1500-m ($\sim$850 hPa) level between 0900 and 1100 UTC 29 December (Fig. 5b), with surface temperature increases between 6° and 10°C in the Puget Sound lowlands observed approximately 14 h later. The precipitation accompanying this front began over the Snoqualmie basin as snow at approximately 0500 UTC 29 December, made a transition to freezing rain as the warm front approached, and then turned to rain after frontal passage. The hydrograph for Carnation showed an increase from a base flow of 80 to over 320 $m^3\ s^{-1}$ in response to this warm-frontal event (Fig. 6c).

Snowmelt and light precipitation sustained the flow on the Snoqualmie River for the next 36 h. Snow depth observations taken at North Bend, near the Cascade foothills, indicate a peak depth of approximately 30 cm (12 in.) at 1200 UTC 29 December. Melting of the snowpack began shortly after warm-frontal passage (0000 UTC 30 December) and continued at a steady rate until about 1200 UTC 31 December, at which time all the snow at North Bend had melted.

A second, strong surface low and associated front passed over the region late on 31 December (Fig. 4b), with precipitation beginning over the Snoqualmie basin at approximately 0000 UTC 1 January and intensifying until the passage of the warm front (Figs. 6a,b). The

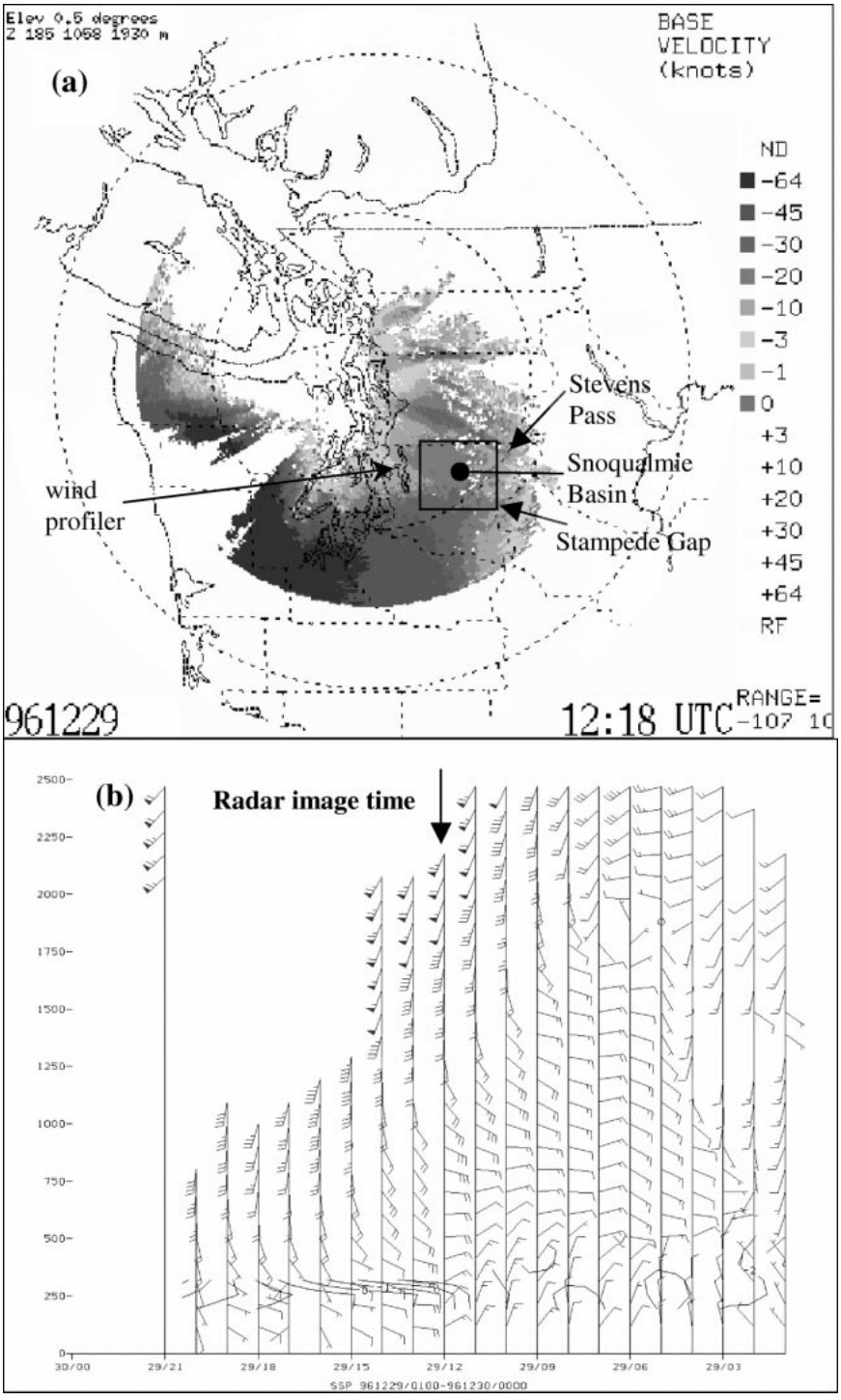

FIG. 5. (a) Radial velocities (inbounds only) from the Camano Island WSR-88D for 1218 UTC 29 Dec. (b) Time series of wind and virtual temperature taken from the Sand Point profiler between 0000 UTC 29 and 0000 UTC 30 Dec. Strong low-level easterly winds are apparent in the regions downwind of the major Cascade gaps in (a), with the flow extending westward to the profiler site.

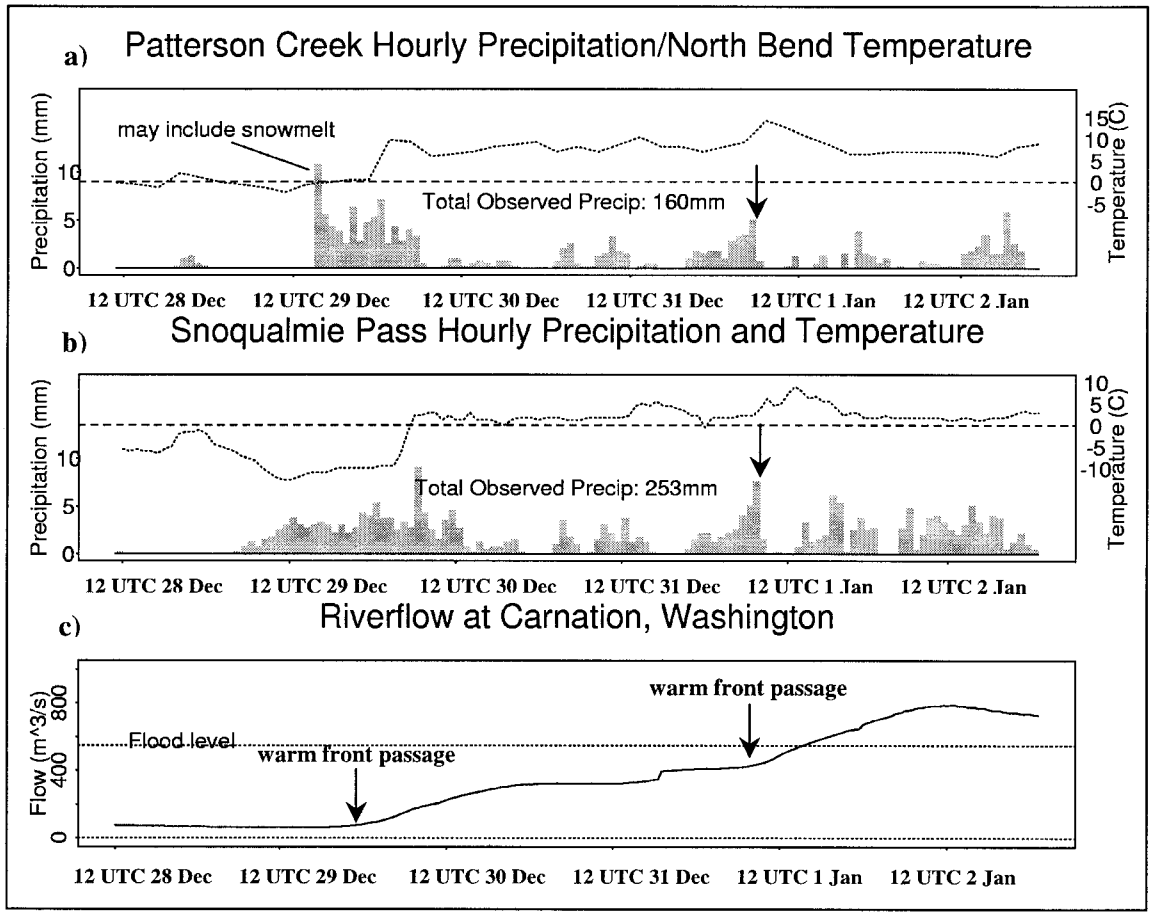

FIG. 6. Observed hourly precipitation at (a) Patterson Creek and (b) Snoqualmie Pass, temperatures (dotted) from (a) North Bend and (b) Snoqualmie Pass, and (c) observed river flow on the Snoqualmie River at Carnation.

WSR-88D showed a line of heavy mixed stratiform–convective precipitation coincident with the front (not shown). Wind shifts from easterly to southerly, strong pressure rises, a brief temperature increase of approximately 3°C, and an abrupt end to the heavy precipitation were coincident with frontal passage (Figs. 6a,b). Following this passage, the weakening of the strong southwesterly flow aloft and the gradual return to cooler temperatures in the higher elevations signaled an end to this ROS flooding event. The peak discharge observed on the Snoqualmie River at the Carnation gauge was 790 $m^3\ s^{-1}$, observed at 1200 UTC 2 January 1997 (Fig. 6c), which is less than or equal to the level of a 2-yr flood (Hartley 1997).

5. Model assessment

a. Synoptic-scale evolution

Comparison of the MM5 initialization with satellite observations over the Pacific Ocean revealed minor discrepancies, but no major problems were identified. However, over land, the simulations between 0000 UTC 28 and 0000 UTC 31 December 1996 had initial model surface temperatures, interpolated from the Eta 104 grids, that were on average 12°C too warm east of the Cascade Range of Washington and Oregon. Radiosonde data (not shown) from Kelowna, British Columbia, located approximately 300 km northeast of the Snoqualmie basin (Fig. 1a), suggested that a cold layer extended to the 850-hPa level (approximately 800 meters above ground level) throughout this 4-day period; this low-level cold air was not captured in the Eta initial fields. However, by hour 12 of the simulations, cold air initialized further to the north and east had moved to the eastern slopes of the Cascades, reducing the surface warm bias east of the Cascades to less than 6°C.

The simulated oceanic cyclones associated with the warm front of 29–30 December and the warm front of 31 December–1 January were within 3 hPa of observed at most times, and position errors were less than 150 km. Despite this apparent skill in forecasting the low's center, both fronts moved too fast over land (not shown). In contrast, the movement of the thermal and wind structures aloft were simulated more accurately. Wind pro-

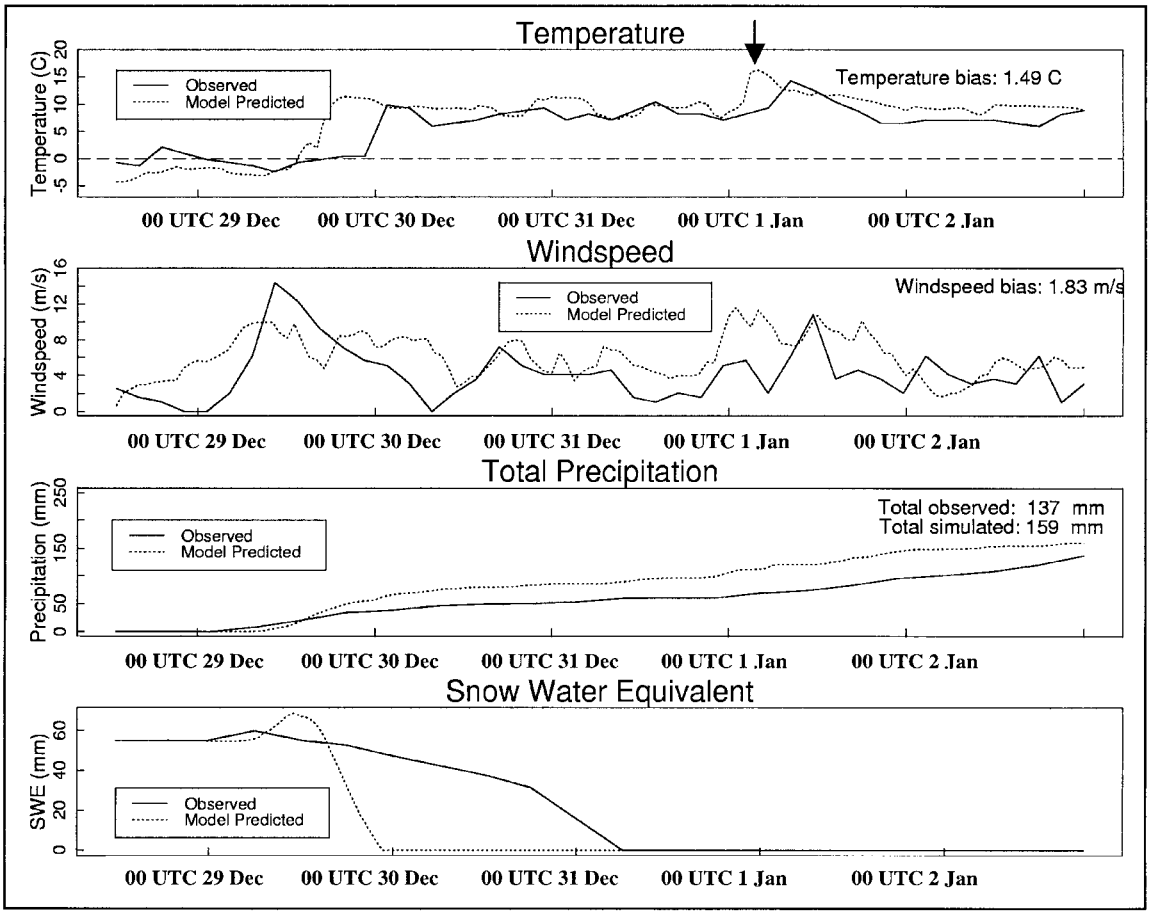

FIG. 7. Time series of temperature, wind speed, precipitation, and SWE for North Bend, WA. SWEs were based on snow-depth observations and assumed snow densities. The arrow denotes the model-simulated warm-frontal passage on 1 Jan 1997.

filer data from Seattle (Fig. 5b) showed a gradual wind shift at 1500 m (approximately the 850-hPa level) from easterly to southerly between 0900 and 1100 UTC on the 29 December. This model wind shift occurred between 0700 and 1000 UTC (not shown), indicating that the front aloft was only 1–2 h too fast, but the surface front ranged from 4 to 7 h too fast at locations throughout western Washington.

b. Low-level winds

Model wind speeds at the lowest sigma level (approximately 40 m) were reduced to 10 m using the logarithmic wind profile (Arya 1988). A time-averaged model high–wind speed bias of approximately 30% was evident in the 4-km simulation in the more mountainous regions, with wind speed biases of 1.8 m s^{-1} at North Bend (Fig. 7) and 2.6 m s^{-1} at Stampede Pass (not shown). In the Puget Sound lowlands west of the Snoqualmie basin, the wind speed bias was not nearly as pronounced, with an event-averaged wind bias ranging between -0.7 and 1.6 m s^{-1}. Comparisons of the average model wind speed bias at 4-, 12-, and 36-km spacing revealed that the model high–wind speed bias increases (worsens) with increasing model grid spacing. For example, the event-averaged wind speed bias for the eight wind observation sites in the Puget Sound region was 0.98, 1.15, and 1.57 m s^{-1} for the 4-, 12-, and 36-km model spacings, respectively.

c. Temperature

Analysis of the MM5 temperature forecasts with available observations revealed that the passage of the warm front of 29–30 December was too fast. Gauges at various elevations in the Snoqualmie Pass area showed that the simulated warming occurred approximately 8 h too early at the 950-m elevation, and 3 h too early at 1645 m (not shown). Surface temperatures at the Olallie Meadow SNOTEL site and at North Bend (Fig. 7a) also showed warming approximately 6 h too early. However, the Alpine Meadows and Skookum Creek (Figs. 8a,b) SNOTEL sites, both located in regions representative of most of the basin (i.e., not located in or downwind of major gaps in the Cascades), show much closer agreement between simulated and

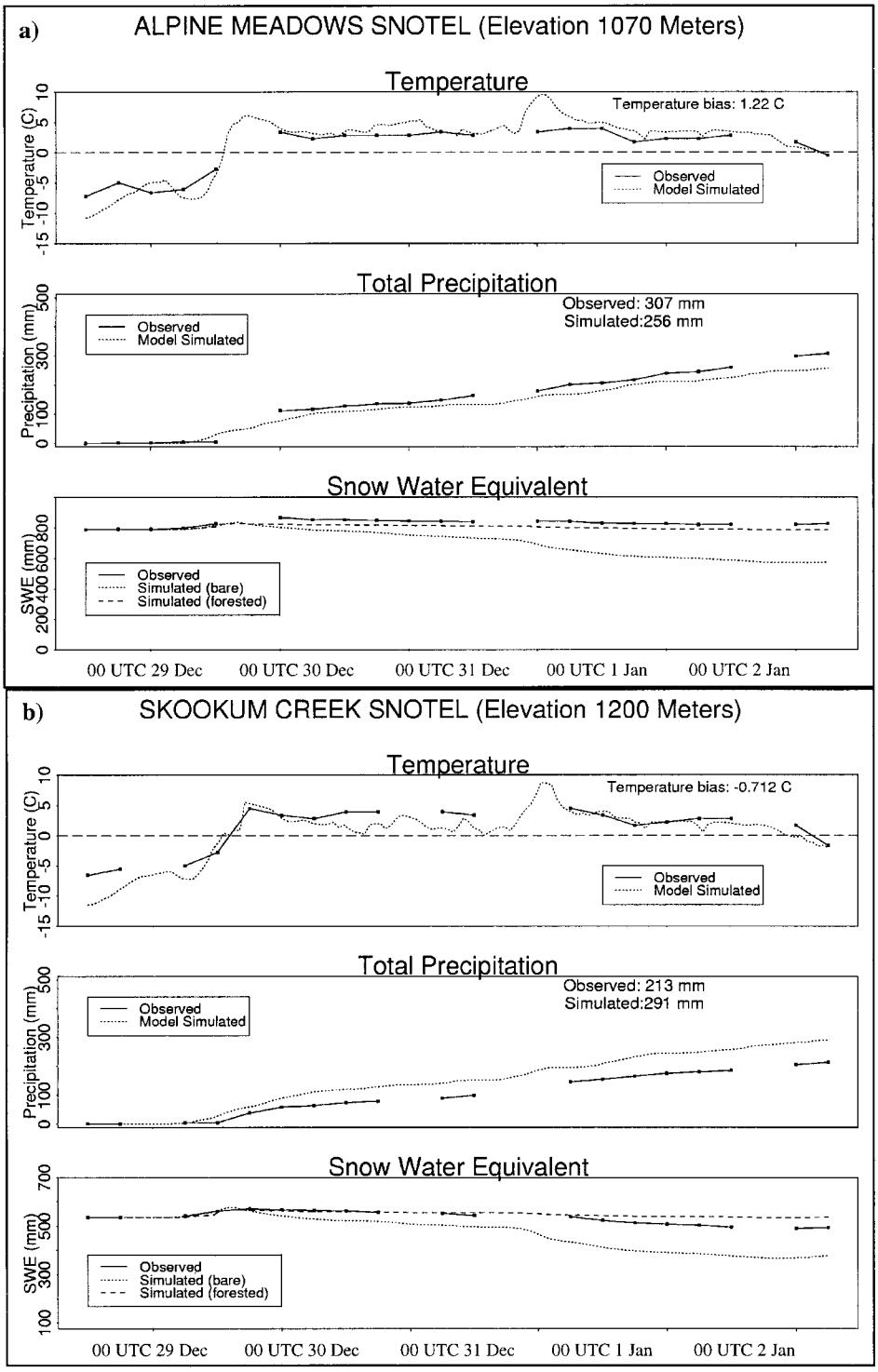

FIG. 8. Temperature, total precipitation, and SWE for the (a) Alpine Meadows and (b) Skookum Creek SNOTEL locations.

observed temperatures. Following this, the model temperatures were well simulated throughout the remainder of the flood event.

Assessment of model temperature predictions with the 35 available observations in the region in and around the Snoqualmie basin showed that temperatures were more accurately simulated at higher resolution, with temperature biases of 0.06°, 1.15°, and 1.13°C for the

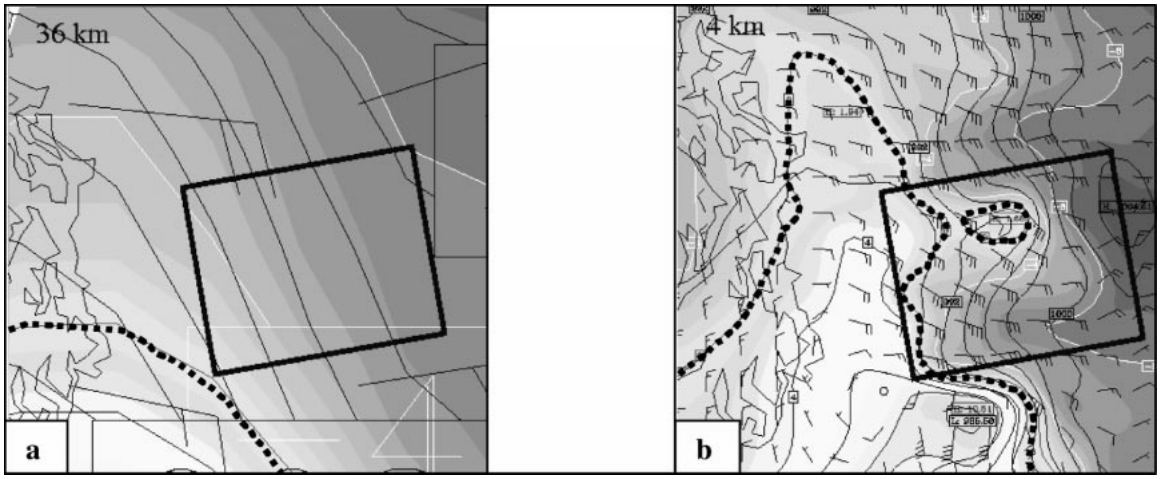

FIG. 9. Comparison of the MM5-predicted temperature and winds for 1200 UTC 29 Dec 1996 at (a) 36- and (b) 4-km spacing. The Snoqualmie basin is outlined in solid, the 0°C isotherm is denoted by a dotted line, cold temperatures are shaded darker, and full wind barbs indicate 10 kt.

4-, 12-, and 36-km-spacing domains, respectively. The 4-km spacing best captured the cold-air outflow from eastern Washington through the Cascade gaps (Fig. 9b), although at all model resolutions the cold air in western Washington was scoured out too quickly.

d. Precipitation

The precipitation at most locations in and near the watershed was underforecast at all model resolutions. A larger-scale evaluation of the precipitation fields (not shown) revealed that the low precipitation bias was most pronounced in the lee of major orographic barriers, in agreement with the results of Colle et al. (1999). Scatterplots of storm total precipitation using the raw rain gauge values (Figs. 10a–c) show that the accuracy of the MM5 precipitation fields varied considerably between the three model resolutions. At 36-km spacing, the storm total precipitation was well simulated over the lower (<200 m) and middle (200–500 m) elevations (denoted by L or M, respectively), but was significantly underforecast for the higher (>500 m) elevations (H), with most locations only capturing 50%–60% of the observed storm total. Improvements at higher elevations occurred when spacing was decreased to 12 km, with this improving trend continuing as spacing decreased to 4 km. The 36-km simulation captured 79% of the observed storm total, the 12-km simulation captured 83%, and the 4-km simulation captured 82%.[1]

The basin-averaged storm total precipitation varied from 148 mm for the 36-km domain to 205 mm for the 4-km domain (Fig. 11a). Even though the 4-km nest produced more precipitation than both the 36- and 12-km nests, it was less than observed. A west-to-east transect of the precipitation distribution across the Cascade crest (Fig. 11b) revealed that over the western (lower) portion of the basin the 36- and 12-km domains have similar amounts of precipitation, but the 4-km grid has approximately 20% less. In the middle and eastern portions of the basin, the 4-km grid shows significantly more precipitation, with a peak (arrow 1) located about 25 km upwind of the crest of the Cascade Range. A less pronounced peak is apparent in the 12-km nest closer to the Cascade mountain crest (arrow 2), and the 36-km domain shows only slight evidence of an upwind peak. The time-averaged upstream peak in precipitation in the 4- and 12-km domains is consistent with previous observational studies (Sinclair et al. 1997; Hobbs et al. 1975). For example, Hobbs et al. showed significant orographic enhancement between crest level and approximately 40 km upwind of the Cascade crest, with a pronounced peak approximately 30 km upwind of the crest, shortly after frontal passage.

e. Snow water equivalent

The combination of high–wind speed and warm-temperature biases led to too rapid ablation of the model snowpack, especially in the lower, nonforested regions. This result was apparent at all model resolutions but, consistent with the wind and temperature biases, was worse at coarser resolution. The low-elevation model snowpack, forced with the 4-km-spacing MM5 fields, had completely melted by 0000 UTC 30 December, but the observed snowpack was not exhausted until 32 h later, at approximately 0800 UTC 31 December (Fig.

[1] Correcting for the effects of gauge undercatchment, using the method of Larson and Peck (1974), reveals that storm total precipitation may have been as much as 12% lower than the raw values. The absence of temperature and wind data at most of the rain gauge locations precluded a more accurate assessment.

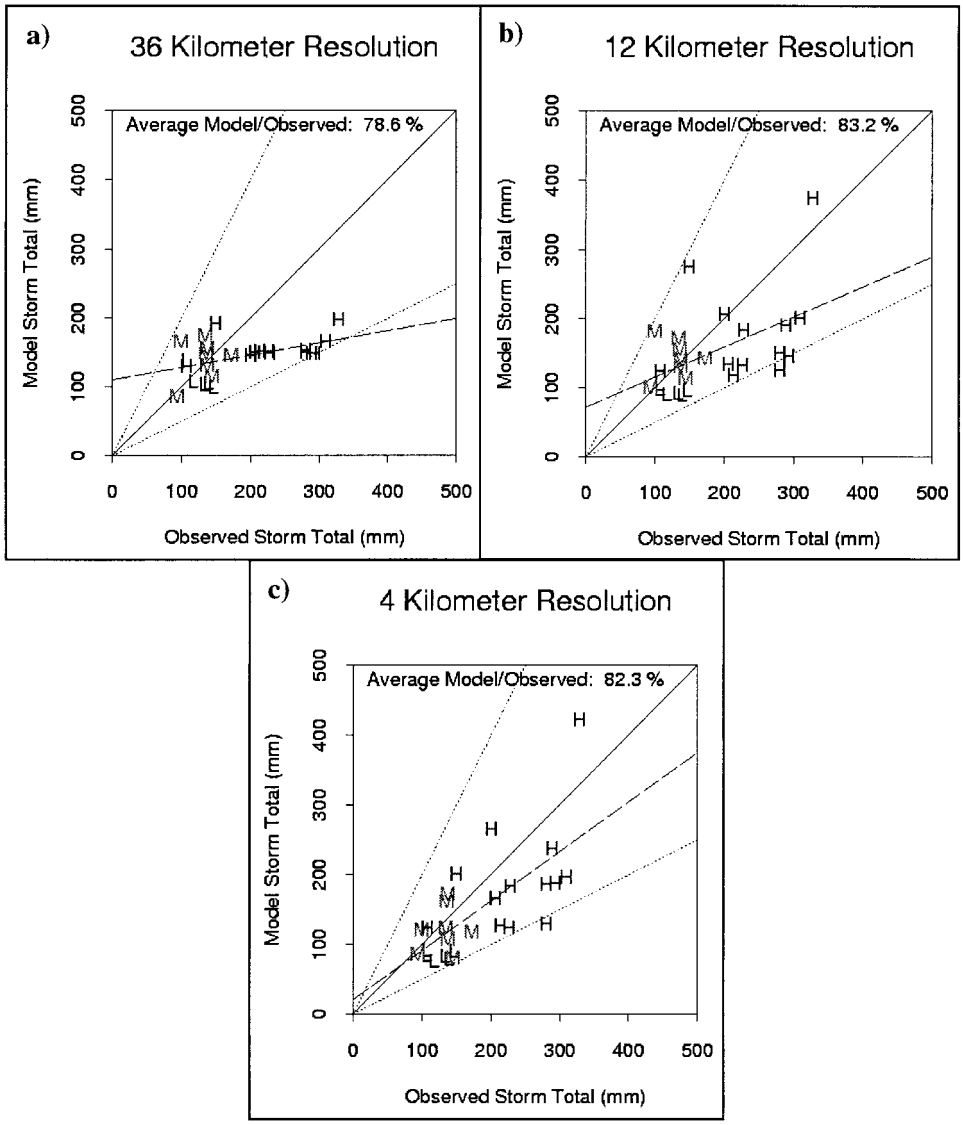

FIG. 10. Storm total precipitation scatterplots for the (a) 36-, (b) 12-, and (c) 4-km MM5 spacings. The high-, mid-, and low-elevation sites are marked H, M, and L, respectively.

7). Time series for the SNOTEL sites show that model SWEs were reasonable when each site was modeled as a small opening in a continuous forest canopy. This designation is consistent with local site conditions, because these SNOTEL sites are located in small (~50 m × 50 m) clear areas within the forest. Thus, they are relatively free of snow interception effects and relatively protected from prevailing winds. Not surprisingly, for an ROS flood event, for which sensible and latent heat transfer dominate snowmelt, accurate representation of the small-scale distribution of vegetation can have a significant effect on predictions of snow ablation. As a comparison, the predicted snow ablation for two of the SNOTEL sites modeled as unlimited clearcuts is shown in Figs. 8a,b.

f. Streamflow

The effects of too little precipitation clearly influenced the predicted peak storm flow at all resolutions (Fig. 12). There is a remarkable degree of similarity in the predicted flows for the various grid resolutions, especially given the aforementioned differences in precipitation. This similarity is a result of a number of compensating factors, including variations in the spatial distribution of model precipitation and model temperature and wind speed biases that affected the rapidity of snowmelt. For example, the 4-km simulation correctly places more of the precipitation in the mid- to high elevations (Fig. 11b), where it is more likely to fall as snow (hence, not available for runoff). In con-

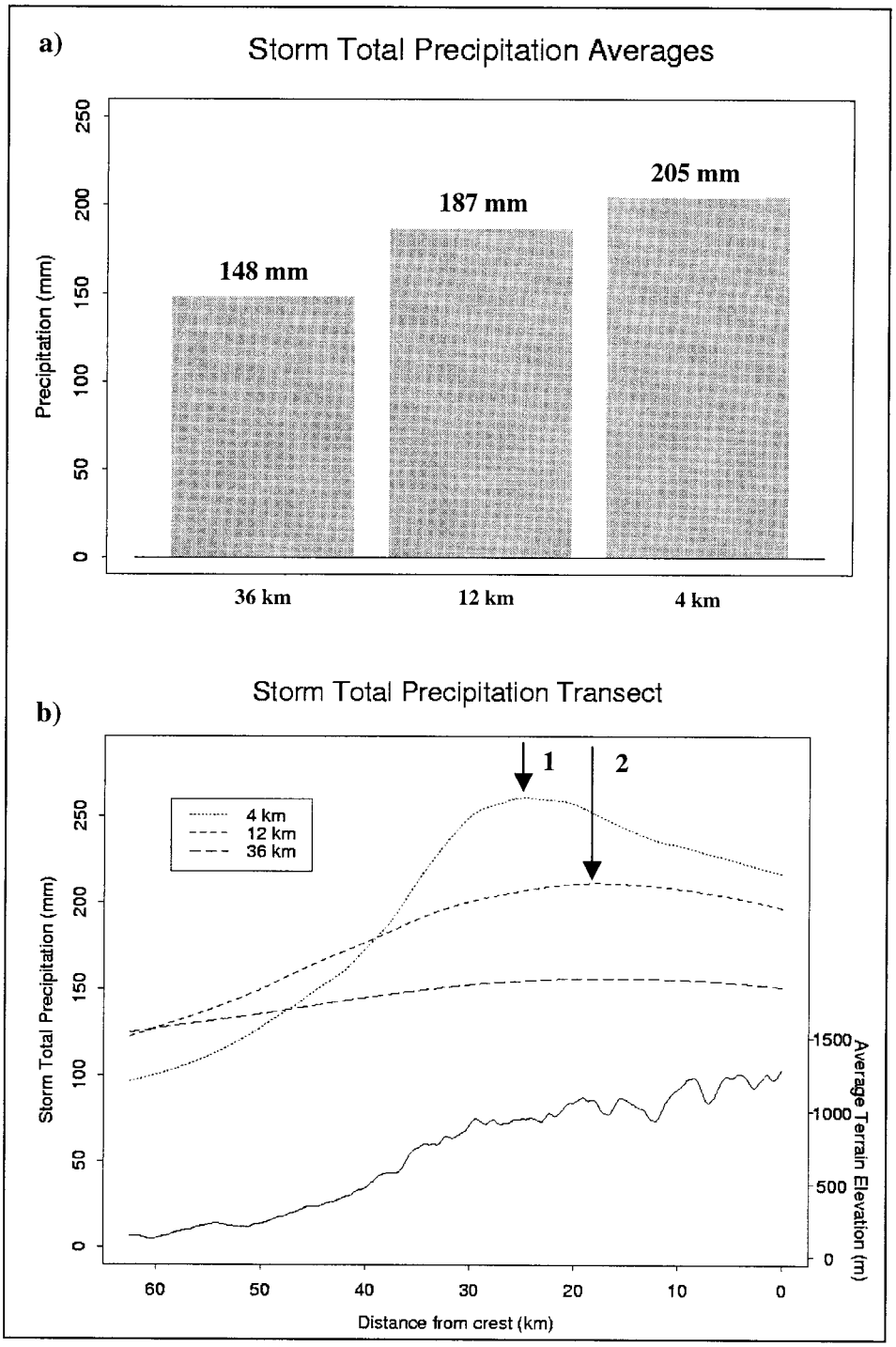

FIG. 11. (a) Model storm total precipitation over the Snoqualmie River basin for the various model resolutions. (b) A west–east transect of the north–south-averaged precipitation over the basin.

trast, the 12- and 36-km domains placed more precipitation in the lower, western third of the basin, where warmer temperatures resulted in the precipitation falling as rain (hence, immediately available for runoff). Also, a majority of the land cover in the western, lower elevations is nonforested, leading to less interception of precipitation. A third reason for the similarity in the simulated streamflows is that the temperature and wind

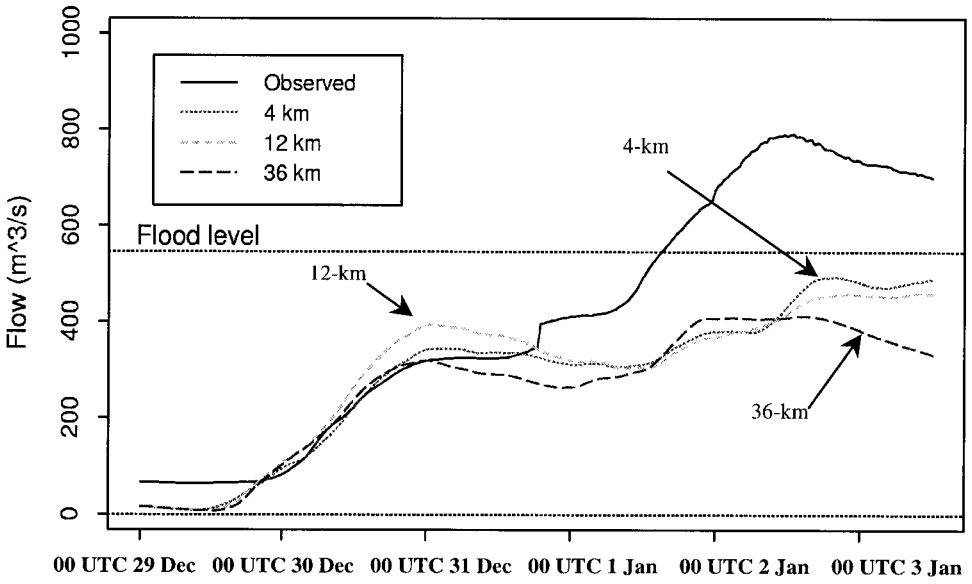

FIG. 12. The observed vs simulated Snoqualmie River flow at Carnation, WA, for the various MM5 control simulations.

speed biases increase (worsen) with decreasing model resolution, causing more rapid snowmelt and greater runoff at coarser resolution.

The 4-km-spacing input produced a peak flow of 493 $m^3\ s^{-1}$, or 62% of the observed (Fig. 12), and was the best resolution for capturing the peak streamflow (Table 1), while the 12-km simulation better captured the total discharge. The 36-km input produced the least amount of flow of all three model resolutions.

6. Sensitivity simulations

a. Rain gauge–enhanced precipitation

The first of the sensitivity simulations used rain gauge data to improve the precipitation fields from the MM5 4-km domain before being used in DHSVM. This sensitivity test was conducted to assess the impact of model precipitation errors on the forecast hydrographs. In addition to being a research question, correcting atmospheric model forecast precipitation with real-time observations could be used for operational forecasting, because the lag between heavy precipitation and flood peak can range from several hours to a few days, depending on the basin size. This spatial correction to the precipitation field was accomplished by first determining an hourly precipitation enhancement ratio (PER), defined as the ratio of observed to simulated precipitation for each observing location in and near the Snoqualmie basin. The PER for any particular time was calculated for a 6-h window centered around the hour

TABLE 1. Results from the various simulations for domain-average storm total precipitation, peak river flow, and storm total discharge.

Simulation	Precipitation [average precipitation over basin (mm)]	Peak flow		Total flow*	
		[peak flow ($m^3\ s^{-1}$)]	[peak flow (percent of actual)]	($\times 10^8\ m^3$)	(Percent of actual)
Observed		791	100	1.80	100
Control (4 km)	205	493	62.3	1.30	72.1
Control (12 km)	187	460	58.2	1.35	74.6
Control (36 km)	148	413	52.2	1.21	67.2
Gauge enhanced (4 km)	247	628	79.4	1.63	90.2
Wind speed reduced (4 km)	247	602	76.1	1.57	86.7
Convective precipitation (4 km)	259	651	82.1	1.68	93.1
Observations-only forcing (precipitation from Snoqualmie Pass and Snoqualmie Falls)	241	494	62.5	0.96	53.3
Observations-only forcing (precipitation from Snoqualmie Pass and North Bend)	187	332	42.0	0.65	34.6

* Reflects the total discharge for the Snoqualmie River at Carnation for the time period of 1200 UTC 28 Dec 1996–0000 UTC 3 Jan 1997.

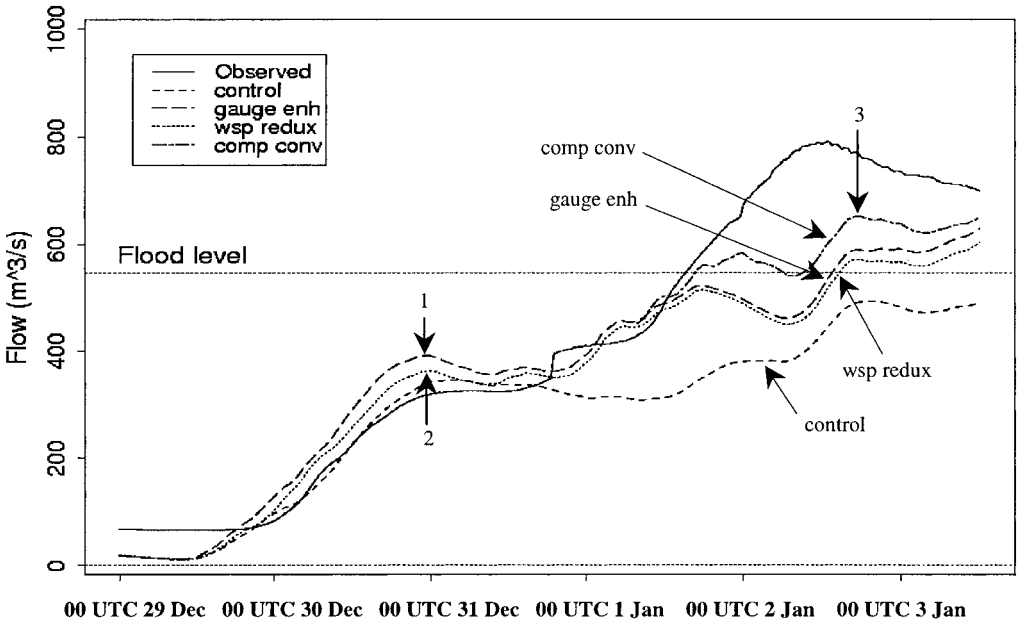

FIG. 13. Observed and simulated river flows for the control, rain gauge–corrected (gauge enh), rain gauge–corrected/30% wind speed reduction (wsp redux), and the rain gauge–corrected/30% wind speed reduction/convective precipitation (comp conv) sensitivity simulations.

in question and was then spatially interpolated to each DHSVM grid point using an elliptic weighting function (Benjamin and Seaman 1985), which stretched the area of influence of the observation in the direction of the wind at the 0.71 sigma level (approximately 700 hPa). The PER values were then multiplied by the MM5 precipitation at every hour for the entire 132-h simulation. After the rain gauge adjustment procedure, the average storm total precipitation within the basin increased to 248 mm, approximately 21% more than in the 4-km control simulation (Fig. 11a). The resulting river flow was substantially improved over the control (Fig. 13, ''gauge enh''), especially after 1 January. The storm peak flow increased to 628 $m^3 s^{-1}$, approximately 80% of the observed maximum, and the storm total discharge reached slightly over 90% of observed (Table 1). This is a significant improvement over the 4-km control simulated peak flow of 493 $m^3 s^{-1}$. The predicted peak flow on 31 December, in response to the rainfall of 29–30 December, increased to 395 $m^3 s^{-1}$ (Fig. 13, arrow 1), slightly greater than both the 4-km control and the observed peak flow.

b. Wind speed reduction

An analysis of the DHSVM snowmelt equations was conducted to assess the snowmelt sensitivity to changes in selected meteorological variables. The parameters were varied around their observed or expected range of error, and the results suggested that the greatest improvements to the model SWE fields would be due to the reduction of the model's positive wind speed bias. Therefore, a sensitivity simulation was completed with a basinwide 30% wind speed reduction applied for the entire 132-h event. Such a reduction essentially removed the time-averaged high–wind speed bias noted in the mountainous regions and is reasonable given the absence of a subgrid-scale orographic drag parameterization in the MM5. This sensitivity simulation also used the rain gauge–enhanced precipitation fields, as described in the previous section.

Modeled snow fields improved substantially after the wind speed reduction, with the simulated SWE at North Bend at 0000 UTC 30 December increasing from 12.2 mm (24% of observed) in the control to 35.9 mm (72% of observed) in the sensitivity simulation. The effect of the reduced snowmelt is also evident on the hydrograph (Fig. 13, ''wsp_redux''), with closer agreement between observed and simulated flow noted in the time period between 0000 UTC 30 and 1200 UTC 31 December 1996 (Fig. 13, arrow 2), the period during which the actual lower-elevation snowpack melted. Reduced flow is also evident after 31 December, indicating that the impact of the winds on snowmelt at higher elevations continued even after the exhaustion of the lower-elevation snowpack.

c. Convective precipitation modification

Figure 14a shows a radar image of the heavy precipitation observed at 0538 UTC 1 January 1997 during the passage of the second warm front. Precipitation rates ranging from 15 mm h^{-1} (40 dBZ) to over 75 mm h^{-1} (50 dBZ) were estimated using the Z–R relationship Z

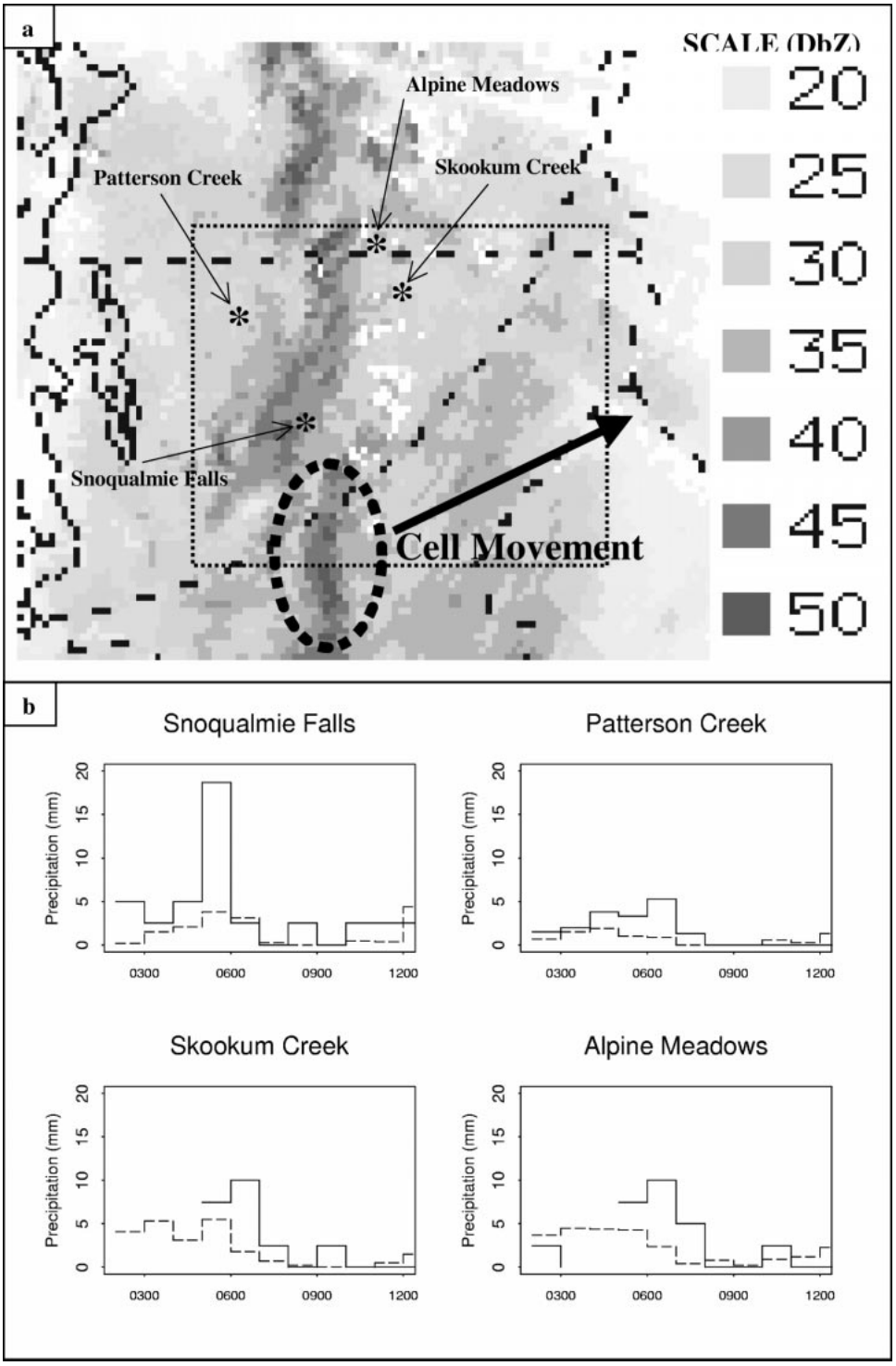

FIG. 14. (a) Radar image for 0538 UTC 1 Jan 1997 detailing the areas of heavy precipitation associated with the second warm-frontal passage. The dashed region shows the location of the Snoqualmie River basin, and the circled region encloses the convective cell that was not accounted for in the convective precipitation modification experiment. (b) Also shown are the modeled (dashed) and observed (solid) hourly precipitation for four locations in the basin.

$= 230R^{1.4}$ (Austin 1987). It can be seen that the high precipitation amounts observed between 0500 and 0800 UTC at the four locations nearest this cell were not captured by MM5 (Fig. 14b), even after the precipitation fields were corrected toward observations. This is partially due to both the use of a 6-h precipitation enhancement ratio and the weighting scheme, which tends to dampen the effects of any short-lived, high-intensity precipitation event. Also, there is a sampling problem, because there are not enough observations to define fully a small-scale convective event.

To assess the effect of this heavy precipitation on the simulated river flow, a convective precipitation field designed to account for the precipitation not captured by the MM5 was created and superposed on the simulated precipitation field for 0700 UTC 1 January. Radar observations from the WSR-88D were used to determine the spatial distribution of the convective precipitation, and available rain gauges were used to determine the amounts. An analysis of the 6-min images from the radar revealed that the intense rainfall lasted between 30 and 60 min, which argues for lumping the convective precipitation into a single 1-h period. Spot checks of the precipitation field before and after the addition of this convective precipitation modification showed much better agreement with observations (not shown). With the convective enhancement, the maximum simulated flow at Carnation increased to 650 $m^3 s^{-1}$, which is 82% of observed (Fig. 13, arrow 3), with a 4-h timing error in the predicted peak.[2]

Despite the significant improvement in both total flow and peak flow, it is still evident that a sizeable amount of runoff is still unaccounted for, principally on 2 January 1997. Close examination of the radar revealed that a second heavy core of precipitation passed over the data-void Middle Fork of the Snoqualmie River (circled in Fig. 14a) between 0530 and 0600 UTC 1 January. Missing data from the Cedar Lake precipitation gauge and the Middle Fork River flow gauge, along with complications from terrain-blocking of the WSR-88D radar beam (the majority of the southeast portion of the Snoqualmie basin is effectively blocked), precluded an accurate assessment of the effects of this cell on river flow.

d. Observations-only forcing (no MM5)

A sensitivity simulation using only observations for forcing (no MM5) was conducted. Stampede Pass and Snoqualmie Falls, the two sites used by Storck et al. (1995), were used as the observation locations. Because of missing precipitation data at several critical times at Stampede Pass, it was necessary to substitute Snoqualmie Pass[3] precipitation data for some periods. Also, the Snoqualmie Falls data were unavailable after 1900 UTC 1 January, after which time the precipitation data from North Bend were used. Both the lower- and upper-elevation observation sites were used to create time-varying temperature and precipitation lapse rates. An inverse-distance method, in conjunction with the derived lapse rates, was used for distributing the precipitation and temperature data over the watershed.[4]

Significant underforecasting of river flow is evident for both events when using only observations for forcing (Fig. 15, ''obs1''), with the discharge for this simulation being 52% of the observed (Fig. 15, arrow 1). The significantly lower peak and storm total flows are surprising given that 241 mm of precipitation fell over the basin (Table 1), considerably more than in any of the MM5 control simulations and much closer to the average precipitation from the simulation that used the MM5 precipitation fields enhanced with the rain gauge observations (247 mm).

Analysis of the snow fields from this simulation (not shown) revealed that the poorly simulated river flow is primarily due to incorrect partitioning of the precipitation between rain and snow. The use of temperatures from North Bend and Stampede Pass caused the basinwide temperatures to be too cold, because temperatures at both locations were greatly influenced by the cold outflow from eastern Washington (Figs. 5a,b). For example, at 2000 UTC 29 December the temperature at North Bend (elev 170 m) was 0°C, and the temperature at the Skookum Creek SNOTEL site (elev 1200 m) was over 4°C. Interpolation of the North Bend temperature over the basin caused nearly all of the model precipitation to fall as snow rather than rain, and, therefore, it was not available for immediate runoff. This temperature effect combined with the precipitation lapse rate method of downscaling the precipitation (which placed more of the precipitation at higher and colder locations) kept runoff fairly low early in the simulation.

The second peak in the hydrograph (Fig. 15, arrow 1) was very similar in timing and predicted peak discharge to the 4-km control simulation. Somewhat fortuitous for this sensitivity simulation was that the intense convective precipitation of 1 January passed directly over the Snoqualmie Falls rain gauge. This single-precipitation value, distributed over much of the basin using the method described above, created a large influx of water in a short period of time. The resulting river flow, while similar to the 4-km results for that period, most likely would have been much less had another nearby observation been used. To show this, a sensitivity simulation using observed precipitation from North

[2] Doug McDonnal, lead hydrologic forecaster at the National Weather Service Forecast Office in Seattle, considers a 4-h error to be an ''accurate'' forecast for the timing of the flood peak at this gauge location.

[3] Snoqualmie Pass is located approximately 20 km northwest of Stampede Pass; both are at the crest of the Cascade Range.

[4] The inverse-distance method was an internal algorithm of the DHSVM version that was used for this study.

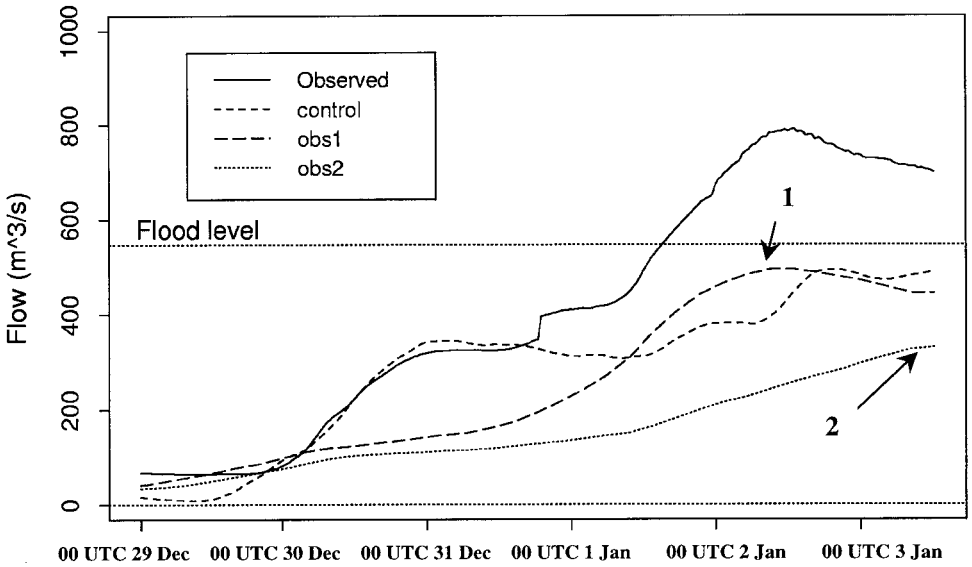

FIG. 15. Observed and model-simulated river flow for the sensitivity experiment using both a lower- and an upper-elevation station for forcing. The simulation obs1 used Stampede Pass (precipitation from Snoqualmie Pass) and North Bend (precipitation from Snoqualmie Falls); simulation obs2 was identical to obs1 except that precipitation from North Bend was used rather than from Snoqualmie Falls.

Bend (8 km from Snoqualmie Falls and not directly in the path of the heavy convective cell) was performed. The resulting river flow (Fig. 15, ''obs2'') captured 34% of the total and 42% of the peak streamflow (Fig. 15, arrow 2), with a significant timing error.

7. Summary and discussion

The PSU–NCAR MM5 mesoscale atmospheric model and the Distributed Hydrology–Soil–Vegetation Model were used to simulate the flooding event of 28 December 1996–3 January 1997. Although this 132-h event was not considered to be a major flood, it did exhibit a number of the complicating meteorological and hydrologic factors, including spatially and temporally variable precipitation, temperature, wind, and snowmelt, that make these events so difficult to predict. The system captured 93% of the total time-integrated flow and over 82% of the peak storm flow, with a 4-h timing error (Table 1), but only after observations were used to enhance MM5 precipitation fields.

The control simulation of the system performed well for the warm-frontal stratiform rainfall event of 29–30 December 1996 at all MM5 model resolutions, but less well for the mixed stratiform–convective precipitation on 1 January 1997, particularly at 36-km spacing. Although a low precipitation bias was evident at all three MM5 resolutions, the volume of water input to the basin in the 36-km grid was significantly less than in either the 12- or 4-km grids. Given the corresponding low simulated streamflow using the 36-km input, it was concluded that the 36-km spacing significantly underpredicted the basin storm total precipitation. This underprediction was at least partially due to poor model representation of the Cascade Range mountain barrier.

Another implication of the poorer model resolution was the inability of the 36-km, and to a lesser degree the 12-km, grid to capture accurately the complex surface temperature and wind patterns, especially the channeling of the cold air through the major gaps in the Cascade Range at the early stages in this event. The coarse model terrain could not resolve the relevant orographic features, with the result that cold temperatures were too widespread over much of the watershed, thus adversely affecting the rain–snow partitioning. This result may have implications for larger-scale modeling studies, because many have focused on the downscaling of precipitation but have otherwise neglected the potentially more difficult question of how best to downscale other relevant meteorological quantities.

The simulated river flow resulting from the first warm-frontal event (between 0000 UTC 30 and 0000 UTC 31 December 1996) was 97%, 106%, and 83% of observed for the 4-, 12-, and 36-km output from MM5, respectively. Although these results are encouraging, analysis of the snow water equivalent and precipitation fields suggests that a too-rapid snowmelt, and the resulting runoff, may have partially compensated for a model low-precipitation bias. A 4-km sensitivity simulation, which reduced both the low-precipitation and high–wind speed bias, yielded an average river flow that was within 2% of observed for this 24-h period.

The control configuration had more difficulty predicting the river flow following the passage of the second warm front on 1 January 1997, capturing between 52% (36 km) and 62% (4 km) of the observed peak

river flow observed on 2 January. Correcting the MM5-predicted precipitation distribution with hourly rain gauge values resulted in simulated peak flow that was nearly 80% of observed, and the storm total flow increased to over 90% of observed. Further augmenting the MM5-predicted precipitation with a limited set of radar-derived precipitation estimates to simulate the effects of a convective line increased the peak flow and total flow to 82% and 93% of observed, respectively. These results show the importance of accurately capturing short-lived, high-intensity convective precipitation, even in the cool season when stratiform-type rainfall is dominant, and underscore the need for integrating radar-derived precipitation estimates into these simulations.

A high–wind speed bias over mountainous terrain (30% overprediction) was identified, although the number of observations used to make this assessment was relatively small. Removal of this bias lead to improvement (reduction) in the model snowmelt, although the reduction in wind speed had a relatively minor effect on the simulated river flow, accounting for only about a 4% change in both total time-integrated and peak flows.

Two sensitivity simulations, using lower- and upper-elevation observations to force the hydrological model (no MM5 forcing), showed considerable sensitivity to the observation locations used. A simulation using an observation that was located under the path of a heavy convective cell captured 53% of the total river flow and over 62% of the peak flow, but when a location only 8 km away was used, the simulation captured just under 35% of the total flow and 42% of the peak flow. Although both simulations had storm total average precipitation values that were similar to those that used MM5 for forcing, the temperatures at these locations were not representative of much of the basin, causing too much of the precipitation to fall as snow rather than rain, resulting in decreased runoff. During this event, the atmospheric model–predicted temperature patterns, which more accurately captured the complex spatial distribution of surface temperatures, were superior to the temperature fields created using the limited set of two observations.

In conclusion, this study showed that there is substantial promise in using high-resolution atmospheric models for directly forcing a distributed hydrological model for forecasting of flood events. It has also shown the potential, and possibly the necessity, of integrating both model- and radar-derived precipitation data, along with point observations, for producing more accurate precipitation and streamflow forecasts.

Acknowledgments. This research was supported by a COMET fellowship grant as well as support from the NOAA Severe Weather Prediction Initiative (Cooperative Agreement NAG7RJ0155) and the National Science Foundation (ATM-9634191). Use of MM5 was made possible by the Microscale and Mesoscale Meteorological Division of the National Center for Atmospheric Research (NCAR), which is supported by the National Science Foundation. Special thanks to Bart Nijssen, Pascal Storck, and Prof. Dennis Lettenmaier from the University of Washington Civil Engineering Department for helpful comments and the use of the DHSVM. A number of people contributed observational data: Erik Moldstad, a private meteorologist, for the observations from North Bend; Luis Fuste of the United States Geological Survey for the observed streamflow data; David Hartley of King County Water and Land Resources Division for the Patterson Creek observations; and Scott Pattee of the NRCS for the SNOTEL observations. The authors also thank Dr. Brian Colle, Mark Albright, Richard Steed, Ernie Recker, Dr. Brad Colman, Doug McDonnal, Dr. Sandra Yuter, and Prof. Robert Houze for their comments and contributions.

REFERENCES

Arya, S. P., 1988: *Introduction to Micrometeorology.* Academic Press, 307 pp.

Austin, P. M., 1987: Relation between measured radar reflectivity and surface rainfall. *Mon. Wea. Rev.,* **115,** 1053–1070.

Benjamin, S. G., and N. L. Seaman, 1985: A simple scheme for objective analysis in curved flow. *Mon. Wea. Rev.,* **113,** 1184–1197.

Bowling, L. C., P. Storck, and D. P. Lettenmaier, 2000: Hydrologic effects of logging in western Washington, USA. *Water Resour. Res.,* **36,** 3223–3240.

Calder, I. R., 1993: Hydrologic effect of land-use change. *Handbook of Hydrology,* D. R. Maidment, Ed., McGraw-Hill, 13.1–13.50.

Colle, B. A., and C. F. Mass, 1996: An observational and modeling study of the interaction of low-level southwesterly flow with the Olympic Mountains during COAST IOP4. *Mon. Wea. Rev.,* **124,** 2152–2175.

——, K. J. Westrick, and C. F. Mass, 1999: Evaluation of the MM5 and Eta-10 precipitation forecasts over the Pacific Northwest during the cool season. *Wea. Forecasting,* **14,** 137–154.

Cressman, G., 1959: An operational objective analysis system. *Mon. Wea. Rev.,* **87,** 367–374.

Dudhia, J., 1989: Numerical study of convection observed during the Winter Monsoon Experiment using a mesoscale two-dimensional model. *J. Atmos. Sci.,* **46,** 3077–3107.

Grell, G. A., J. Dudhia, and D. R. Stauffer, 1995: A description of the Fifth-Generation Penn State/NCAR Mesoscale Model (MM5). NCAR Tech. Note NCAR/TN-398 + STR, 122 pp. [Available from UCAR Communications, P.O. Box 3000, Boulder, CO 80307.]

Hartley, D., 1997: Snoqualmie River basin—Water year 1997 flood summary report. King County Water and Land Management Internal Rep., 9 pp. [Available from Customer Account Services, King County Water and Land Resource Division, 201 S. Jackson St., Suite 600, Seattle, WA 98104; or online at http://dnr.metrokc.gov/hydrodat/FloodReports/Snoqual97.html.]

Hobbs, P. V., R. A. Houze, and T. J. Matejka, 1975: The dynamical and microphysical structure of an occluded frontal system and its modification by orography. *J. Atmos. Sci.,* **32,** 1542–1562.

Kain, J. S., and J. M. Fritsch, 1990: A one-dimensional entraining/detraining plume model and its application in convective parameterization. *J. Atmos. Sci.,* **47,** 2784–2802.

Katzfey, J. J., 1995: Simulation of extreme New Zealand precipitation events. Part I: Sensitivity to orography and resolution. *Mon. Wea. Rev.,* **123,** 737–754.

Larson, L. L., and E. L. Peck, 1974: Accuracy of precipitation mea-

surements for hydrologic modeling. *Water Resour. Res.,* **10,** 857–863.

Maidment, D. R., J. F. Olivera, A. Calver, A. Eatherall, and W. Fraczek, 1996: A unit hydrograph derived from a spatially distributed velocity field. *Hydrol. Processes,* **10,** 831–844.

Martin, G., 1996: A dramatic example of the importance of detailed model terrain in producing accurate quantitative precipitation forecasts for southern California. Western Region Tech. Attachment 96-07, National Weather Service, 9 pp. [Available from Western Regional Climate Center, Desert Research Institute, 2215 Raggio Parkway, Reno, NV 89512.]

McQueen, J. T., R. R. Draxler, and G. D. Rolph, 1995: Influence of grid size and terrain resolution on wind field predictions from an operational mesoscale model. *J. Appl. Meteor.,* **34,** 2166–2181.

Miller, N. L., and J. Kim, 1996: Numerical prediction of precipitation and river flow over the Russian River watershed during the January 1995 storms. *Bull. Amer. Meteor. Soc.,* **77,** 101–105.

Sinclair, M. R., D. S. Wratt, R. D. Henderson, and W. R. Gray, 1997: Factors affecting the distribution and spillover of precipitation in the southern Alps of New Zealand—A case study. *J. Appl. Meteor.,* **36,** 428–442.

Stauffer, D. R., and N. L. Seaman, 1994: Multiscale four-dimensional data assimilation. *J. Appl. Meteor.,* **33,** 416–434.

Steenburgh, J. W., C. F. Mass, and S. A. Ferguson, 1997: The influence of terrain-induced circulations on wintertime temperature and snow level in the Washington Cascades. *Wea. Forecasting,* **12,** 208–227.

Storck, P., D. P. Lettenmaier, B. A. Connelly, and T. W. Cundy, 1995: Implications of forest practices on downstream flooding. Phase II final report. University of Washington Rep., 100 pp. [Available from WFPA, 724 Columbia St. NW, Suite 250, Olympia, WA 98501.]

——, L. Bowling, P. Wetherbee, and D. Lettenmaier, 1998: Application of a GIS-based distributed hydrology model for prediction of forest harvest effects on peak stream flow in the Pacific Northwest. *Hydrol. Processes,* **12,** 889–904.

Taylor, G. H., 1997: The Great Flood of 1996. Oregon State University Report, Oregon State University. [Available from Oregon Climate Service, Oregon State University, Strand Ag Hall, Room 316, Corvallis, OR 97331.]

Urbonas, B. R., and L. A. Roesner, 1993: Hydrologic design for urban drainage and flood control. *Handbook of Hydrology,* D. R. Maidment, Ed., McGraw-Hill, 28.1–28.52.

van Heeswijk, M., J. S. Kimball, and D. Marks, 1996: Simulation of water available in clearcut forest openings during rain-on-snow events in the western Cascade of Oregon and Washington. Water Resources Investigations Rep. 95-4219, U.S. Geological Survey, 67 pp. [Available from Information Services, U.S. Geological Survey, Box 25286, Federal Center, Denver, CO 80225.]

Warner, T. T., D. F. Kibler, and R. L. Steinhart, 1991: Separate and coupled testing of meteorological and hydrological forecast models for the Susquehanna River basin in Pennsylvania. *J. Appl. Meteor.,* **30,** 1521–1533.

Westrick, K. J., C. F. Mass, and B. A. Colle, 1999: The limitations of the WSR-88D radar network for quantitative precipitation estimation over the coastal western United States. *Bull. Amer. Meteor. Soc.,* **80,** 2289–2298.

Wigmosta, M. S., L. W. Vail, and D. P. Lettenmaier, 1994: A distributed hydrology–soil–vegetation model for complex terrain. *Water Resour. Res.,* **30,** 1665–1679.

Zhang, D. L., and R. A. Anthes, 1982: A high-resolution model of the planetary boundary layer—Sensitivity test and comparisons with SESAME-79 data. *J. Appl. Meteor.,* **21,** 1594–1609.